A HIGH TEMPERATURE FUSION REACTOR DESIGN

by

S. D. Harkness, J. F. dePaz, M. Y. Gohar and H. C. Stevens

Prepared for

14th Intersociety Energy Conversion Engineering Conference

Boston, Massachusetts

August 5-10, 1979

ARGONNE NATIONAL LABORATORY, ARGONNE, ILLINOIS

Operated under Contract W-31-109-Eng-38 for the

U. S. DEPARTMENT OF ENERGY

A HIGH TEMPERATURE FUSION REACTOR DESIGN

S. D. Harkness, J. F. dePaz, M. Y. Gohar and H. C. Stevens
Argonne National Laboratory
Argonne, Illinois 60439

ABSTRACT

Fusion energy may have unique advantages over other systems as a source for high temperature process heat. A conceptual design of a blanket for a 7 m tokamak reactor has been developed that is capable of producing 1100°C process heat at a pressure of ∿ 10 atmospheres. The design is based on the use of a falling bed of MgO spheres as the high temperature heat transfer system. By preheating the spheres with energy taken from the low temperature tritium breeding part of the blanket, 1086 MW of energy can be generated at 1100°C from a system that produces 3000 MW of total energy while sustaining a tritium breeding ratio of 1.07. The tritium breeding is accomplished using Li_2O modules both in front of (6 cm thick) and behind (50 cm thick) the high temperature ducts. Steam is used as the first wall and front tritium breeding module coolant while helium is used in the rear tritium breeding region. The system produces 600 MW of net electricity for use on the grid.

BACKGROUND

Fusion energy has several advantageous features as a source of high-temperature process heat when compared with other possible sources. First, it is based on inexhaustible fuels sources (deuterium and lithium) that do not have significant non-energy applications. This is an important advantage over fossil-based fuels. Second, a far greater fraction of the energy is carried by the neutron than in fission processes (80 versus 5%). This presents an inherent means of transporting the energy from the nuclear reaction zone to a high-temperature region that can be isolated from contamination by radioactive species inherent to the nuclear process. This advantage of fusion over fission is further enhanced by the fact that the neutron emitted by the (d,t) reaction is considerably more energetic than is a fission neutron (14 versus 2 MeV).

This paper summarizes an effort to develop an engineering design for a high temperature (> 1000°C) fusion reactor. The design effort is based on the use of a tokamak fusion source that has a major radius of 7 m, an aspect ratio of 3, an assumed β_t of 0.07, a plasma elongation factor, κ, of 1.8, and a thermal output of 3000 MW. All the reactor design parameters were chosen as a result of previous efforts (1) to produce the most economical, least technologically complicated design.

The blanket design took as its basis four major goals. These were: (1) The capability to produce process heat at a temperature in excess of 1000°C. (2) The development of a design that would allow the direct use of a non-activated process heat stream without recourse to the use of a high-temperature heat exchanger as a means of isolating the primary coolant loop due to concerns over transported radioactivity. (3) The elimination of ceramics as structural materials in the reactor. (4) The system should be nearly self-sustaining with respect to tritium breeding and this should be done in a way to ensure no contamination of the process heat stream.

The approach to a high-temperature fusion reactor blanket design suggested by this report attempts to avoid the problems of static designs through the use of a ceramic falling bed. As a high-temperature blanket concept, the falling bed is particularly attractive in that it allows the decoupling (2) of the structural materials from the high-temperature heat transfer medium. As shown in recent studies, (2,3) by actively cooling the structural walls, modest temperatures (∿ 500°C) can be maintained while producing a high (> 1000°C) temperature in the falling ceramic pellets. From a feasibility point of view, this may prove much more reasonable than would the construction of an integral structure capable of withstanding 1000°C temperatures. Such a system also minimizes the pumping requirements to a few hundred kilowatts of power due to the fact that it can be operated at low pressures. Because of the high density of the falling particle bed compared to more conventional coolants, a relatively small volume throughput is sufficient to absorb the energy output of a fusion reactor. For example, if Al_2O_3 is used as the coolant media at an entrance temperature of 300°C and an exit temperature of 1000°C, a throughput of less than 2 tons per second is required to absorb an output of 1000 MW of thermal energy.

NEUTRONIC ANALYSIS

The main neutronic design considerations for the falling bed high-temperature fusion blanket concept are the energy fraction deposited in the high temperature region, the tritium breeding ratio, the induced radioactivity, the afterheat, and the biological hazard potential. A major objective of the high temperature fusion blanket design is to facilitate the deposition of as large a fraction of the neutron fusion energy in the high temperature region as possible. The falling bed high-temperature fusion blanket concept can be designed such that from 0.90 to 0.95 of the total available energy is deposited in the high temperature region if the tritium breeding is sacrificed. The tritium breeding issue can be looked at in two different scenarios. The first scenario requires a tritium breeding ratio adequate for self-sufficiency while the second does not require self-sufficient tritium breeding (tritium breeding < 1.0) because tritium will be available from other operating reactors in a mature fusion economy. The present design is based on the first scenario, that requires a tritium breeding ratio greater than one.

A one-dimensional transport analysis has been conducted in a parametric fashion so as to scope and

define the potential of various design possibilities. This neutronic study was conducted so as to determine the following parameters as a function of design geometries and material selection: (a) tritium breeding ratio; (b) energy (both absolute and fraction of total) deposited in the high-temperature bed; (c) induced radioactivity in the system; (d) the rate of atomic displacement and gas generation as a function of material selection, and (e) the shield characteristics of the blanket design.

The neutronic calculations were conducted in terms of the schematic shown in Figure 1. Three different breeding materials; liquid lithium, Li_2O and Li_7Pb_2 were included in the assessment along with MgO, Al_2O_3 and SiO_2 as candidate pellet materials. Stainless steel was assumed to be the structural material and a carbon reflector was also included.

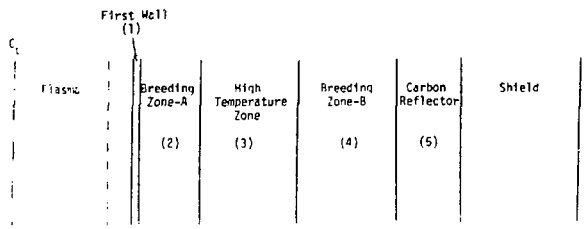

(1) Type 316 stainless steel, 3-mm thick.

(2) 10% stainless steel, 5% coolant (H_2O or He), 85% breeder (Li or Li_7Pb_2).

(3) 75% of theoretical density of Al_2O_3, MgO or SiO_2.

(4) 10% stainless steel, 5% coolant, 85% breeder.

(5) 5% stainless steel, 5% coolant, 90% carbon.

Fig. 1. A schematic of the blanket model used for the parametric neutronic analysis.

The performance of several representative blanket designs is presented in Table 1. The key points to be noted from this study include: (1) Tritium breeding ratios near 1 can be achieved for any of the combinations of breeder and pellet materials while depositing a minimum of 25% of the total energy in the high-temperature zone. A maximum deposition of 51% of the total energy was achieved in one of the designs. (2) The total energy produced by the system was higher when MgO or Al_2O_3 beds were chosen instead of SiO_2. (3) For a given system, the choice of MgO or SiO_2 resulted in higher tritium breeding ratios than did Al_2O_3. (4) The use of H_2O instead of He as a structural coolant gave relatively higher tritium breeding ratios and lower fractions of the total energy deposited in the high-temperature bed.

A multiregional blanket design approach has been adopted to insure that the bred tritium will be kept separate from the high temperature region.

The radioactivity analysis for different blanket designs was performed using the DHR code (4). The use of water as a coolant resulted in slightly lower radioactivity levels (3%), biological hazard potential (2.5%), and afterheat (2.6%) compared to using helium as a coolant. Table 2 shows a sample of the radioactivity results for three identical blankets that use different high temperature materials. The radioactivity in the high temperature region shows a minimum with SiO_2 in comparison with Al_2O_3 and MgO after 10^6 seconds from the shutdown. The principal contributor to the induced activity in the Al_2O_3 and MgO cases is Na-24.

A three dimensional Monte Carlo calculation was performed for the reference design that accounted for both spatial and material selection changes. Figure 2 shows the reactor blanket geometry used in the Monte Carlo calculations. It should be noted that the top and the bottom of the reactor are not used for high temperature deposition. The thickness of the inner blanket, high temperature region is half the thickness of the outer one. Table 3 shows the integral results from the Monte Carlo calculations for the three different high-temperature materials. The

Table 1. The Neutronic Performance of a Number of High Temperature Fusion Blanket Designs

Blanket Number	C1	C2	D1	D2	E1	E2	B1	B2	F1	F2	G1	G2
Breeder Material	Li_7Pb_2	Li_7Pb_2	Li_7Pb_2	Li_7Pb_2	Li_7Pb_2	Li_7Pb_2	Li_7Pb_2	Li_7Pb_2	Li_2O	Li_2O	Li_2O	Li_2O
Coolant	H_2O	H_2O	H_2O	H_2O	H_2O	H_2O	He	He	He	He	H_2O	H_2O
High Temperature Material	Al_2O_3	Al_2O_3	MgO	MgO	SiO_2	SiO_2	Al_2O_3	Al_2O_3	MgO	MgO	MgO	MgO
Breeder Thickness, cm	5/45	10/45	5/45	10/45	5/45	10/45	5/45	10/45	5/45	10/45	5/45	10/45
High Temperature Zone, Thickness, cm	40	40	40	40	40	40	40	40	40	40	40	40
$^6Li(n,\alpha)T$ Reaction/DT Neutron	0.931	1.097	0.962	1.135	0.959	1.131	0.906	1.067	0.774	0.838	0.767	0.831
$^7Li(n,n'\alpha)T$ Reaction/DT Neutron	0.105	0.165	0.108	0.165	0.116	0.172	0.108	0.169	0.210	0.317	0.214	0.325
Tritium Breeding Ratio	1.036	1.262	1.070	1.300	1.075	1.303	1.014	1.236	0.984	1.155	0.981	1.156
Energy Deposition in the Beds MeV/DT Neutron	8.6	5.7	8.2	5.3	6.7	4.3	9.02	6.24	7.47	4.38	7.69	4.63
Total Energy Deposition MeV/DT Neutron	17.8	17.9	16.9	17.0	16.6	17.0	17.82	17.97	17.33	17.59	17.33	17.6
Energy Fraction Deposit in the High Temperature Region	0.48	0.32	0.48	0.33	0.40	0.25	0.51	0.35	0.43	0.25	0.44	0.26

Table 2. Biological Hazard Potential and Radioactivity Resulting from the Choice of Three Different Ceramic Materials

Time After Shutdown (s)	BHP of the High-Temperature Region, Km^3/Km		
	Al_2O_3	MgO	SiO_2
0	1.50E + 02	8.73E + 01	2.47E + 01
10^2	1.18E + 02	8.30E + 01	1.24E + 01
10^3	7.14E + 01	8.09E + 01	4.29E - 01
10^4	6.08E + 01	7.16E + 01	1.29E - 01
10^5	1.91E + 01	2.25E + 01	1.65E - 04
10^6	3.94E - 03	2.14E - 04	---
10^9	3.77E - 03	---	---
10^{11}	3.76E - 03	---	---

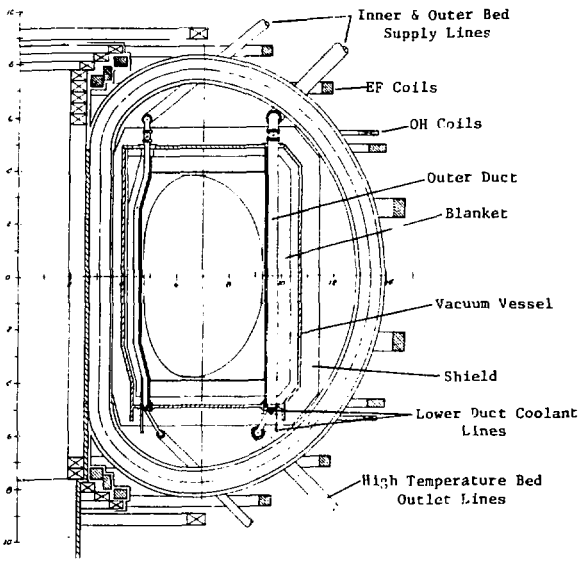

Fig. 2. A cross section of the high temperature tokamak reactor.

results show that the maximum breeding ratio is achieved with MgO and SiO_2. The SiO_2 deposits the lowest energy per fusion neutron in the system and the lowest fraction of energy in the high temperature region.

Based on the above analysis and material considerations, MgO was selected as the reference pellet material. The water coolant with solid breeder is excluded from the reference design based on safety considerations. Liquid lithium was not considered for a similar reason. This left either He or steam as the coolant as the primary choice with Li_2O as solid breeder. Li_2O was selected over Li_7Pb_2 because of the desire to use part of the energy generated in the

Table 3. Three Dimensional Results for Three Different High Temperature Materials for the Reference Design

	MgO	Al_2O_3	SiO_2
Total breeding ratio	1.07	1.05	1.07
Total energy/DT neutron	19.08	19.12	18.16
Energy deposition in the high-temperature region/DT neutron	6.50	7.08	5.03

tritium breeding region to preheat the ceramic pellets prior to their introduction to the reactor blanket. This is done to maximize the amount of energy that the system produces at 1100°C. The use of the higher outlet temperature afforded by the higher melting point Li_2O (in comparison with Li_7Pb_2) is important in achieving this objective.

THERMAL-HYDRAULIC ANALYSIS

The thermal analysis of the pebble bed and heat exchanger system requires the investigation of two related phenomena: the gravity flow of the pebbles, and the transfer of heat through and out of the pebble bed. This investigation has yielded values for several design parameters and suggested a configuration for the walls of the falling bed blanket.

It has been established that the rate of particle flow can be controlled by a suitable design of the outlet orifice, and the velocity of the pebbles is almost constant throughout the bin volume, with only a 10% decrease in the vicinity of the walls. Also, the pressure forces acting at the bottom of the bin increase with bed height only up to a certain point, reaching a saturation value when the bed height equals 2-1/2 times the bin diameter. This is expected to maintain the compression load on the pebbles within acceptable limits. No major problems are anticipated that would preclude the use of gravity bulk flow in the system. The pebble size is determined by considerations of pressure drop and thermal stresses. Small pebble sizes result in pressure drops higher than the weight of the bed, thus impeding the pebble flow, while large particles may experience excessively high thermal stresses during their circulation through the heat exchanger. The pebble diameter has been tentatively chosen as 1.27 cm. The velocity of the gas stream in the heat exchanger is, of course, a major factor determining the pressure drop in the heat exchanger, and its value has been chosen as 1.5 m/s. This results in a pressure drop which is about one fifth of the pressure drop that would be required to support the bed. Calculations of the rate of heat transfer between the pebbles and the coolant have shown that the solid and gas reach thermal equilibrium within a short distance from the inlet; this is due, primarily, to the large heat exchange surface per unit volume that results from the packed bed geometry. Consequently, the outlet temperature of the gas will approach the inlet temperature of the pebbles and the heat exchanger height will be determined by the residence time required for sufficient decay of the pebble radioactivity and by the geometric characteristics that would result in uniform downflow of the pebbles. If the inlet steam temperature is taken to be 120°C and its outlet temperature 1090°C, then the limitations on the steam velocity require a heat exchanger cross-sectional area of 51 m^2 (assuming

twelve such heat exchangers are provided). A heat balance then yields a value of ∿ 0.06 m/min for the pebble velocity inside the heat exchanger and a height of 8.0 m would result in a residence time of 133.0 min.

As stated above, part of the heat produced in the breeding blanket will be used to pre-heat the pebbles, raising their temperature from 150°C to 450°C in a pre-heater placed above the high-temperature region. The addition of this pre-heating stage makes it possible to increase the pebble throughput for a given outlet pebble temperature, thus increasing the high-temperature heat ouptut by 45%. The solid stream will be pre-heated with steam at ∿ 3 atmospheres in twelve pre-heaters having a cross-sectional area of 35 m^2.

The heat transfer and temperature distribution analysis of the falling bed is based upon a two-dimensional finite difference solution of the energy equation. Correction factors are then applied to the results given by this model to take into account the heat losses through the small sides of each bin. The pebble bed and brick walls are subject to a volumetric heat generation that decreases exponentially with distance. The brick wall lining the duct exchanges heat with the steel panels through a gap, while the steel panels are kept at a low constant temperature by active cooling. The heat transfer inside the bed is governed by an equivalent bed thermal conductivity (4,5) while the bed exchanges heat with the wall by the two additive mechanisms of convection (described in terms of a heat transfer coefficient given by ref. 6) and radiation. The pebble velocities were obtained by iteration, such that the outlet bulk temperature was always 1090 ± 11°C. The resulting pebble velocities are of the order of 0.5 m/min.

Besides those mentioned above, the following parameters were adopted to define a base case: a neutron wall loading of 2 MW/m^2, and a ceramic wall thickness of 2.5 cm. Temperature distribution and heat flows were then computed to identify potential problem areas and the base case parameters were varied in order to establish the best feasible design. Three different ceramic materials (Al_2O_3, MgO and SiO_2) were considered. The gap between the ceramic wall and the steel panel was initially taken to be 0.13 mm, is as expected for normal contact between the brick and the steel panel; it was also assumed at the outset that the pebble velocity would be constant throughout the bed. The amount of heat lost to the actively cooled steel panels is determined by the magnitude of the heat generation in the pebbles, wall and panels, and the thermal resistance of these three regions and the wall-panel gap. The overall thermal efficiency of the falling bed blanket is shown in Fig. 3 as a function of wall loading.

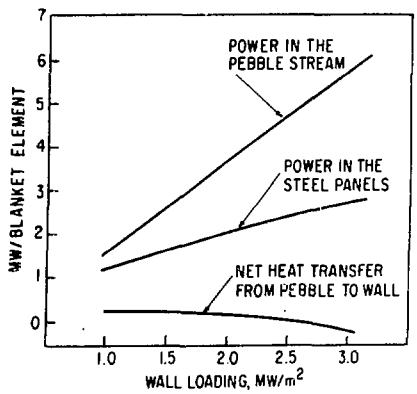

Fig. 3. The partitioning of power in an unimproved falling bed duct.

The relative proportion of heat carried by the pebble stream is larger for the higher wall loadings. This is due to an increase with wall loading of the amount of heat transferred from the brick wall to the falling bed at the top of the blanket. (It is found that the temperature of the brick wall is higher than that of the pebbles in that region so that some of the heat generated in the wall is convected away by the pebbles. Note also that the brick wall heat generation increases with wall loading, whereas the pebble inlet temperature is taken to be constant.) Calculations performed with thinner walls and a constant blanket thickness showed a decrease in thermal efficiency. It appears that an increase in pebble bed volume is offset by the larger amount of heat loss through the thinner wall. Figure 4 shows the pebble and wall temperatures as a function of heat load. The melting point of the ceramic material is reached for wall loadings of ∿ 2.5 MW/m^2. Thus, relatively high heat losses and pebble and wall temperatures were found to be two potential problem areas. In order to reduce the heat losses, the original design was modified, increasing the gap between the ceramic brick and steel panel. This increases the thermal resistance of the wall assembly. It was also found advisable to introduce a thin metal layer in the gap in order to decrease the radiative losses. A lowering of the maximum temperatures (and also a further increase in the thermal efficiency) was achieved by dividing the pebble bed into two regions of different pebble velocity by means of a partition wall. Figure 5 shows the temperature distribution at the bottom of the blanket with and without partition. In the two region case a higher pebble velocity has been adopted on the left-hand side to compensate for the higher volumetric heat generation in it. In this way, a significant reduction has been achieved in the maximum temperatures. This, in turn, results in some reduction of the heat losses. Table 4 summarizes the thermal performance of the above described designs. The highest thermal efficiency presented (corresponding to the case of 12% heat losses) is not a final figure, but rather an indication of the improvement in thermal characteristics resulting from the proposed design modifications, and can be further upgraded by an increase in the power density and/or blanket size.

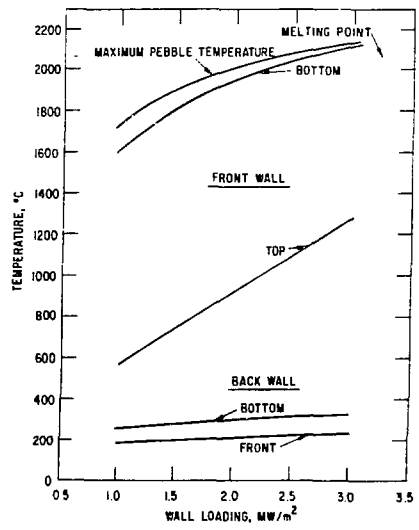

Fig. 4. Temperature profiles within an unimproved falling bed duct.

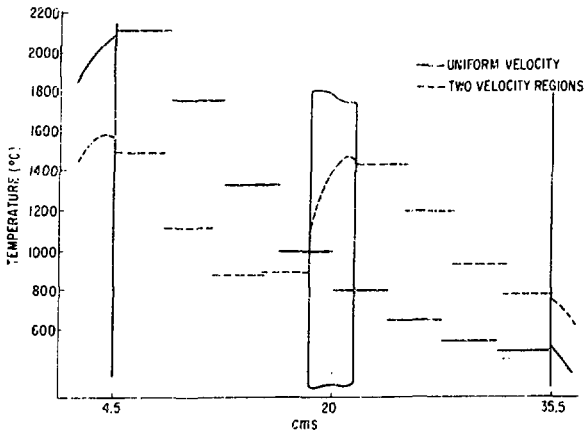

Fig. 5. The effect of velocity partitioning on the temperature profiles within within a falling bed duct.

Table 4. The Effect of Duct Design on the Heat Loss and Pebble Temperature

	Heat Loss to Steel Panels (%)	Maximum Temperatures (°C) Pebbles	
Base Case	25	1943	2005
12.7 mm gap and shield	15	2078	2099
12.7 mm gap with two velocity regions	12	1455	1438

MECHANICAL DESIGN

The major features of the high temperature falling bed tokamak reactor are categorized into three systems; the high temperature, MgO process heat system, the first wall/tritium breeding blanket system and the steam energy conversion system. The neutronic analysis of the system design developed through the use of the previous thermal-hydraulic analysis indicates that the plasma energy is deposited in the various reactor components yielding 1086 MWt of 1090°C MgO pebbles for process heat, 1920 MWt of first wall blanket coolant heat suited for conversion in a conventional steam cycle to 730 MWe gross with a net power to the grid of 635 MWe. In addition, the reactor breeds tritium at a ratio of 1.07.

HIGH TEMPERATURE, MgO SYSTEM - This system consists of a two zone annular inner and outer vertical falling bed duct arrangement as shown in Fig. 6 which are sandwiched between two tritium breeding regions. These high temperature ducts are joined and manifolded at the base of the reactor into twelve loops, with each loop containing; a high temperature MgO to air or steam process heat exchange, a conveyor device to lift the cooled spheres back to the top of the reactor, a steam MgO preheater, and all interconnecting duct and rotary seal valving. The conveyor device contains a screening device for removing pellet fragments and a mechanism for adding makeup spheres. The entire system is enclosed and kept in a controlled atmosphere at all times (see schematic Fig. 6). The MgO spheres enter the lower conveyor at 150°C traveling up to the preheater where they pick up 320 MW of heat leaving at 425°C and enter the reactor bed ducts where they gain an additional 766 MW exiting at 1100°C with a net available energy of 1086 MW.

The reactor ducts may be seen in Figs. 7 and 8. The inner duct is 0.6 M wide x 0.2 M thick in cross-section, 8 M high (active). It is shown in elevation with a slight "C" shaped offset which conforms to the plasma profile and is so designed to facilitate vertical removal between TF magnet coils. There

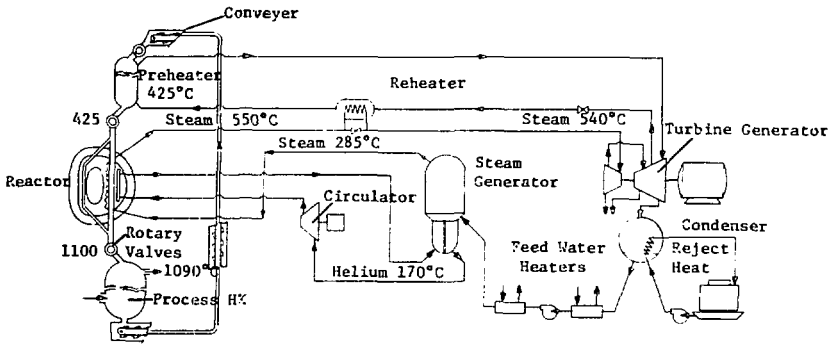

HIGH TEMPERATURE PROCESS HEAT SYSTEM

	REACTOR	PREHEATER	PROCESS HX
TIN,°C	425	150	1100
TOUT,°C	1100	425	150
MW,Th	766	320	1086

HELIUM BLANKET COOLING SYSTEM

		REACTOR	PREHEATER	T-C
	170	285	425	540
	500	550	225	-
	1510	778	320	765 MWe GROSS

NET PROCESS HEAT - 1086 MW,Th

NET ELECTRIC OUTPUT - 660 MWe

Fig. 6. High temperature reactor system schematic.

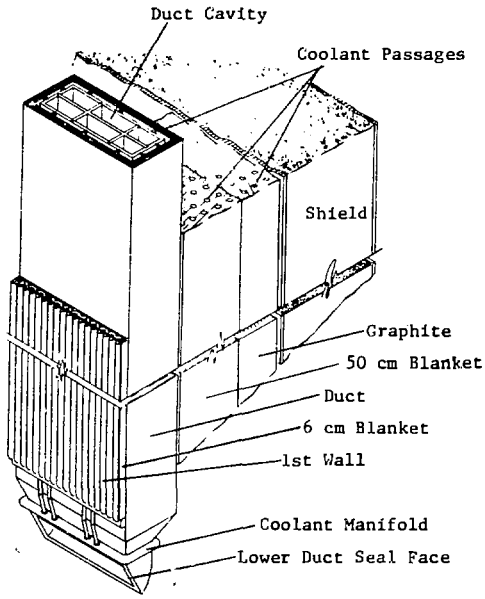

Fig. 7. Outer blanket duct arrangement.

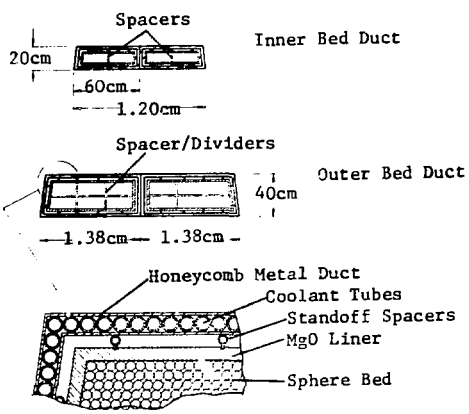

Fig. 8. High temperature reactor duct arrangement.

are 48 of the inner type ducts forming an annular ring in the blanket. The outer ducts are designed in two width sizes; 0.85 meters and 1.37 meters by 0.40 m thick and 8 m high. These ducts are straight in contrast to the inner duct and are partitioned to accommodate the variation in energy distribution. The ducts extend from a bottom support/flange in the lower shield to the top of the reactor vacuum vessel cover. Forty eight ducts, half of which are 0.85 m and half 1.37 m in width, make up a barrel like vertical annulus about the reactor outer blanket with twelve spaces of 0.85 m in width distributed between each of the TF coils. These spaces permit entry of the vacuum ports, neutral beam injection/rf heating and fuel injection. The ducts themselves consist of a ferritic stainless steel pressure tight container made up of a honeycomb section of longitudinal tubes sandwiched between two plates welded into an 8 m long rectangular duct. The honeycomb construction provides the necessary structural rigidity while the tubes act as both spaces and coolant channels. There are longitudinal coolant tubes mounted on the inner wall surface at intervals with inward facing fins which act as spacers to the internally contained MgO liner. The fins are intermittent to minimize heat losses. The lower portion of the duct is necked down on all four surfaces to tapered support fitting beneath which is a rectangular/oval disconnect flange. The indentation in the lower duct is used to house the coolant distribution manifolding that serves both the duct, the plasma face 6 cm thick breeding blanket and the first wall which are attached and supported by the duct. The top fitting is a horizontal oval flange with direct access for disconnect and removal equipment. The ducts are free standing and designed to withstand net internal pressures of up to 10 atmospheres.

The inside of the ducts are lined with an insulating contoured rectangular section of fired 1.5 cm thick MgO tiles which stand off from the duct walls 1 cm positioned by the aforementioned cooled spacer tubes. A spacer/divider grid is fitted into the outer 40 cm thick duct while spacers only are used in the inner 20 cm duct. The liners, spacers and dividers are to be constructed in 40 to 60 cm lengths and slid into the duct from the upper opening. The liners and internals are supported at the bottom and are free to expand upward with temperature while the stand-off spacers are designed to fit tightly at hot operating conditions.

In operation, steam coolant is introduced into the bottom manifold of the ducts at 285°C and flows upward leaving the duct at about 550°C while removing some 114 MW of heat, most of which is due to radiative heat loss from the high temperature bed system.

SYSTEM AND OPERATION - The cavities within the MgO liners provide the path ways for the MgO spheres which enter from 12 distribution points above the reactor through a rotary seal which is pressure balanced and bled to minimize leakage and operated at 425°C. From the upper rotary seal the spheres are fed into insulated, gravity-fed, piping manifolds from which they travel downward into the reactor ducts which are sealed from the reactor vacuum system. The gas atmosphere within the reactor is taken as helium with an alternate of steam. The spheres enter the reactor at 425°C and absorb 766 MW net of neutron heat exiting at 1200°C with a total energy of 1086 MW (320 MW from the preheater). Twelve packed bed heat exchangers (8 m dia. x 8 m high) receive the exiting high temperature bed at the rate of 100 tons/minute. The cooled spheres, 150°C, leave the process heat exchanger through a pressure balance seal falling onto an enclosed gas tight conveyor system operating at slightly positive pressure where they are elevated some 65 m to the preheater. Prior to entering the preheater, the spheres enter a low temperature 150°C rotary seal, pressure balanced to operate up to 50 psig. The spheres then enter one of twelve 6 m diameter x 5 m high preheaters where 320 MW of heat is transferred from steam bled from a low pressure stage (< 50 psig of the turbine and superheated to 425°C). Here the bed is at 425°C ready for entry to the reactor completing the cycle. Ancillaries of this system include MgO dust and particle collection systems, damaged sphere removal and replacement systems, conveyor and rotary valve power and pressure balance systems.

FIRST WALL BLANKET SYSTEMS - The constituents of the outer vertical first wall/blanket/bed/shield system are shown in Fig. 6 and consist of a tubular panel coil first wall section ~ 1.5 cm thick; a 6 cm

thick Li_2O plasma face blanket section; the 40 cm thick high temperature duct; a 50 cm Li_2O-helium cooled blanket; a 30 cm carbon zone followed by the shield. The first wall and 6 cm blanket are of major interest as they are integrated with the high temperature duct for support, coolant, and removal/replacement procedures. The first wall is a welded set of corrugated plates joined together to form a row of full length vertical coolant passages covering an area 8 m high by up to 1.35 m in width in a single panel assembly. The material choice is a ferritic stainless steel. The panel is headered top and bottom to a steam supply and return manifold attached to the high temperature duct. A series of restraints that permit differential expansion secure the panel to the adjacent 6 cm blanket section. Steam coolant enters the first wall panel at 285°C and travels upward to the top exiting at $\sim$ 550°C at a pressure of 1000 psig. A total of 470 MW of plasma α energy is removed from the first wall panels in this manner.

A 6 cm Li_2O breeder section is placed between the first wall panel and the duct. This layer of sintered tritium breeder material, Li_2O, is canned in the above mentioned candidate first wall material and is interspersed with vertical coolant tubes running parallel to those in the first wall and duct. The contained Li_2O is purged with high purity helium for tritium extraction at near atmospheric pressure while the coolant tubes carry steam at 1000 psig entering at 285°C exiting at $\sim$ 550°C removing plasma neutron heat. This blanket unit is also hooked up to the duct steam supply and return manifolds. It is attached mechanically to the duct on one side and the first wall on the other allowing for differential expansion of all pieces. These three interconnected components are removed from the reactor as a single unit with a common support and coolant system, with a dual set of small helium/tritium extraction lines.

ENERGY SYSTEMS - Aside from the described high temperature falling bed system which produces the major product 1086 MW of 1100°C process heat, at from 1-10 atmospheres in pressure, there is a helium blanket cooling system utilizing 1510 MW of breeding blanket heat and a reactor steam system generating 778 MW of heat (of which $\sim$ 320 MW are put into the high temperature region through the preheater). Residual heat not used in the high temperature system is utilized in a conventional modern steam plant to generate electricity delivering a substantial net surplus to the grid.

A helium system similar to those used for the HTGR fission reactor is herein proposed (see Fig. 5). Heat is generated in the reactor's major Li_2O tritium breeder modules consisting of canned blocks of sintered Li_2O interlaced with parallel flow small diameter coolant tubes. Helium at 70 atmospheres ($\sim$ 1000 psi) enters the blocks through a distribution heater at 180°C and exits at 500°C where it flows to a steam generator depositing 1510 MW of heat. It leaves the steam generator at $\sim$ 170°C and enters a circulator requiring 90 MW to provide the required head capacity. All components utilized in this system have been developed and should be reliable with modest refinement.

The steam cooling system coupled with the helium represents a modified dual cycle system where the helium deposited energy is used to generate steam at 285°C, 1000 psig which is then sent to the reactor high temperature subassemblies where it is superheated to 550°C and sent on for process bed (320 MW) and to the turbine (1968 MW). The turbine inlet steam temperature is $\sim$ 525°C equivalent to modern turbine conditions at 1000 psig. With these conditions, energy conversions efficiency of 39% are reasonable yielding a 765 MWe gross output. The losses are estimated at 105 MWe including a 33 MW requirement for reactor power (cryogenics, power supplies, neutral beams, etc.) which place the net electrical output at 660 MWe

ACKNOWLEDGEMENTS

This study benefited from discussions held with M. M. Hall and M. D. Rechtin on material selection and with R. Clemmer on tritium breeding schemes. The editing and typing of the manuscript by Ms. Carolyn Poore is gratefully acknowledged.

REFERENCES

1. M. A. Abdou, et al., "Parametric System Analysis for Tokamak Power Plants," Argonne National Laboratory, ANL/FPP/TM-100, November, 1977.

2. D. K. Sze, I. N. Sviatoslavsky, E. T. Cheng and K. I. Avci, "Thermal Mechanical and Neutronic Design Considerations for a Graphite Structure Li_2O Cooled Blanket," University of Wisconsin, UWFDM-223, October, 1977.

3. H. C. Stevens, M. M. Hall, Y. Gohar, J. F. dePaz and S. D. Harkness, "Fusion Energy for Alternative Applications: The Design of a High-Temperature Falling Bed as a Long-lived Blanket," Argonne National Laboratory, ANL/FPP/TM-117 (1979).

4. D. Kunii and M. Suzuki, "Heat Transfer Between Wall Surface and Packed Solids," Third International Heat Transfer Conference, Chicago, August, 1966.

5. S. Yagi and D. Kunii, "Studies on Effective Thermal Conductivity in Packed Beds," AIChE Journal, 3, No. 3, p. 373, 1957.

6. A. O. O. Denloye and J. S. M. Botterill, "Heat Transfer in Flowing Packed Beds," Chem. Eng. Sci. 32, p. 461, 1977.